

Lawrence Berkeley National Laboratory

Lawrence Berkeley National Laboratory

Title

Film quantum yields of EUV & ultra-high PAG photoresists

Permalink

<https://escholarship.org/uc/item/0883m83x>

Author

Hassanein, Elsayed

Publication Date

2008-03-15

Film Quantum Yields of EUV & Ultra-High PAG Photoresists

Elsayed Hassanein,¹ Craig Higgins,¹ Patrick Naulleau,¹ Richard Matyi,¹ Gregg Gallatin,² Gregory Denbeaux,¹ Alin Antohe,¹ Jim Thackeray,³ Kathleen Spear,³ Charles Szmanda,³ Christopher N. Anderson,⁴ Dimitra Niakoula,⁴ Matthew Malloy,⁵ Anwar Khurshid,⁵ Cecilia Montgomery,⁵ Emil C. Piscani,⁵ Andrew Rudack,⁵ Jeff Byers,⁶ Andy Ma,⁵ Kim Dean⁶ and Robert Brainard¹

¹ College of Nanoscale Science and Engineering, University at Albany, NY 12203

² Applied Math Solutions, LLC; ³ Rohm and Haas Microelectronics, Marlborough, MA 01752

⁴ Center for X-Ray Optics, Lawrence Berkeley National Laboratory, Berkeley, CA 94720

⁵ SEMATECH, Albany, NY 12203; ⁶ SEMATECH, Austin, TX 78741

ABSTRACT

Base titration methods are used to determine C-parameters for three industrial EUV photoresist platforms (EUV-2D, MET-2D, XP5496) and twenty academic EUV photoresist platforms. X-ray reflectometry is used to measure the density of these resists, and leads to the determination of absorbance and film quantum yields (FQY). Ultrahigh levels of PAG show divergent mechanisms for production of photoacids beyond PAG concentrations of 0.35 moles/liter. The FQY of sulfonium PAGs level off, whereas resists prepared with iodonium PAG show FQYs that increase beyond PAG concentrations of 0.35 moles/liter, reaching record highs of 8-13 acids generated/EUV photons absorbed.

Keywords: EUV, Film Quantum Yield, EUV-2D, Base Titration, Photoresists, Ultrahigh PAG Resists

1. INTRODUCTION

As the semiconductor industry continues to follow Moore's Law, the demand to print ever smaller features continues. Extreme ultraviolet (EUV) lithography is the leading candidate for 22 nm half pitch manufacturing. Despite recent advances in EUV resists, simultaneously achieving the required resolution, line-edge roughness (LER) and sensitivity remains a significant issue for EUV (Figure 1).¹ We refer to the competing nature of these three crucial elements as the RLS trade-off.² Gregg Gallatin and coworkers²⁻⁴ have described the nature of the RLS trade-off using an analytical model. In Gallatin's work, as well as that of our own,⁵ predictions have been made suggesting that the best way to get the required resolution, LER, and sensitivity all in the same resist is by creating more acid/photon absorbed (increased film quantum).

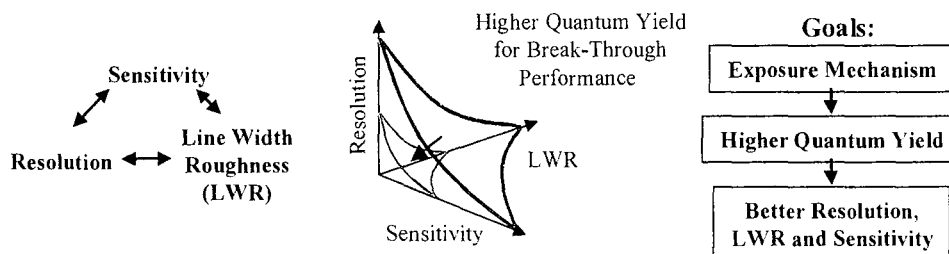


Figure 1. Trade-off between three principal resist performance targets.

We define the film quantum yield (FQY) as the number of acids generated in the film divided by the number of photons absorbed by the film (Figure 2). We assert that this quantity is a useful measure of the effectiveness of a given exposure process since it is an important indicator of LER and RLS performance⁴ and is more appropriate than the quantum yield as traditionally defined in photochemistry. In traditional photochemical experiments, a compound is dissolved in a transparent solvent and irradiated. Photochemical reactions can, thus, be traced back to the absorption of a single photon by a single molecule. In EUV exposures, however, all components of the resist participate in the absorption of the light and interact with the photoelectrons,⁶⁻¹³ therefore, we study the absorption and acid generation in the whole film and call this ratio, the “film quantum yield” to distinguish it from the conventional photochemical definition.

(A) **Film Quantum Yield** = $\frac{\text{Number of Acids Generated}}{\text{Number of Photons Absorbed by Resist Film}}$

(B)

Resist	Exposure Wavelength		
	248 nm	193 nm	13.5 nm
EUV-2D	0.33	0.14	2.08

Figure 2. (A) Definition of film quantum yield. (B) Film quantum yield of EUV-2D at three wavelengths.⁵

One of the simplest and most efficient ways to explore quantum yields and the RLS trade-off is to prepare and evaluate a series of resists with different base levels.¹⁴ Accordingly, we have evaluated five resist platforms with multiple base loadings for a total of thirty resists (Table 1) using EUV lithography at two SEMATECH facilities (Albany EUV MET (AMET) and Berkeley EUV MET (BMET)). We determined C-parameter, optical density and acid quantum yield for each resist platform.

Platform	Resist	Polymer Type	Source	
1	EUV-2D (XP5435D)	High Ea Phenolic	RHEM	} RLS Limitations Model
2	MET-2D (XP5271D)	High Ea Phenolic	RHEM	
3	XP-5496	Low Ea Phenolic	RHEM	
4	Published Resists	High Ea Phenolic	CNSE	
5	Ultra-high PAG Resists	High Ea Phenolic	CNSE	} Ultra-High PAG

Table 1. EUV resist platforms investigated.

Here, we describe our work in three parts. First, we characterize three Rohm and Haas EUV resists in support of the Gallatin-Naulleau-Brainard RLS limitation modeling work supported by SEMATECH.²⁻⁴ Next, we evaluate the FQY of a resist system previously described by Intel, MIT-LL and NIST.¹⁵⁻¹⁸ One advantage of this system is that we can specifically describe all of the components of the resist. We present the FQY as a function of PAG loading and the work is also in supports the development of Gallatin's RLS model.²⁻⁴ Lastly, in platform 5, we describe resists with ultrahigh levels of PAG and evaluate the C-parameter and FQY at these elevated PAG levels.

2. RESULTS and DISCUSSION

2.1 RLS Support

2.1.1 Quantum Yield of EUV-2D. In previous work,⁵ we demonstrated that the film quantum yield of the well known resist, EUV-2D is 2.08 using the 10X2 EUV exposure tool at Sandia National Labs in Livermore, CA. To ensure that the experiments done recently on the AMET and BMET were consistent with the experiments done originally, we repeated the earlier experiments with EUV-2D. The resist was screened for dose-to-clear at AMET (contrast curves, Figure 3A) and imaged at BMET, printing 50 nm 1:1 dense lines to establish Esize. We found that there was a correlation between AMET Eo and BMET Esize where BMET Esize = 2X AMET Eo. Indeed, the typical Esize/Eo ratio on the BMET is 2.0.¹⁹ We plotted the old and new data for comparison (Figure 3B). In our original work, we described the film absorbance by measuring the film density at NIST.²⁰ In our recent experiments, we used the X-ray reflectometry instrument at the College of Nanoscale Science and Engineering (CNSE) as described in the experimental. We determined the film quantum yield using the BMET Esize method, and the AMET Eo method to be 2.13 and 1.94, respectively. We consider the conclusions from all of these experiments to be essentially the same—two acids are generated for each photon absorbed by a 125 nm film of EUV-2D.

Exposure tool	Year	Tk (nm)	Density *	OD (CXRO) nat log	Transmittance	C-Parameter (cm ² /mJ)	Quantum Yield
10X2 at Livermore	2000	125	1.15	4.11	0.592	0.0514	2.08
B MET (Esize/2)	2007	125	1.26	4.54	0.567	0.0507	2.13
A MET (Eo)						0.046	1.94

Table 2. Original and New Results of EUV Quantum Yield of EUV-2D resists. * Density measurements were made by NIST in 2000,²⁰ and by CNSE in this paper.

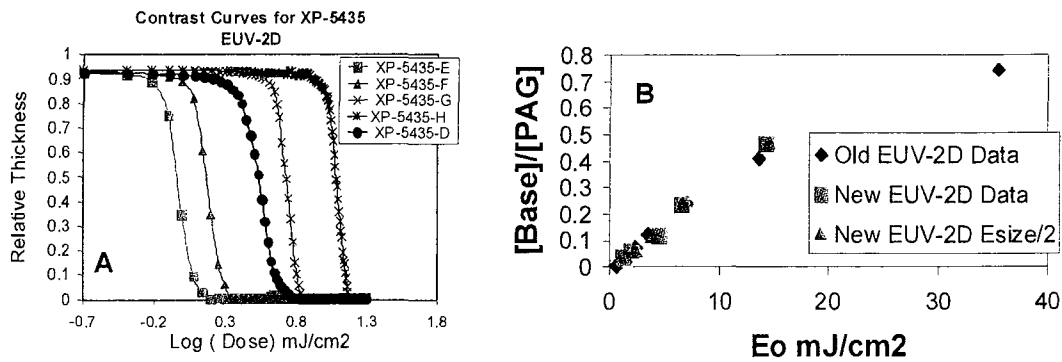


Figure 3. (A) Contrast curve plots for EUV-2D as determined using the AMET. (B) Comparison of C-Parameter plots for EUV-2D as determined originally in 2000 at Sandia National Labs (Old) and determined at the end of 2007 on the AMET and BMET.

2.1.2 Quantum Yield of Platforms 1-3: EUV-2D, MET-2D and XP5496 Resists. In addition to EUV-2D, we have also evaluated high and low activation resist materials from Rohm and Haas to characterize the correlation between the quantum yield and polymer type. The low activation resist, XP5496, was processed using a post-exposure bake (PEB) of 100 °C, whereas, the high activation resists EUV-2D and MET-2D (XP5271) used PEB temperatures of 130 °C. Table 3 contains the experimental results of film density, the corrected C-parameters, and the calculated film absorbance and film quantum yield. Both of these new resists (MET-2D and XP5496) show lower C-parameters and lower film quantum yields. These lower values are probably a result of thinner film thickness used.

Resist	Abs/1 μm	Film Thickness (nm)	Transmittance (Actual Thickness)	C-Parameter (cm ² /mJ)	Density (g/cm ³)	Quantum Yield
XP5435D EUV-2D	4.54	125	0.57	0.046	1.26	1.94
XP5271D MET-2D	4.37	80	0.71	0.0152	1.2	1.39
XP-5496	4.68	80	0.56	0.0167	1.21	1.45

Table 3. Quantum Yield for Platforms 1-3.

2.2 Published Resist Formulations

Figure 4 shows the chemical compounds described previously¹⁵⁻¹⁸ and used in our platform 4 (published resists) and platform 5 (ultrahigh PAG resists). We prepared custom formulations of two chemically amplified (CA) resist systems: ESCAP with either TBPI-PFBS or with TPS-PFBS as a PAG. We used an ESCAP terpolymer in combination with tetrabutyl ammonium hydroxide (TBAH) solution initially prepared as an ethyl lactate master batch. The solvent was a 50/50 blend of ethyl lactate and propylene glycol monomethylether acetate (PMA).

Twelve resists were prepared with 5, 7.5 and 10% iodonium PAG loading and four levels of base (Table 4). Clearing dose (Eo), corrected C-parameter and film quantum yield as a function of PAG loading are shown (Figure 5). As expected, the resists get faster with increasing [PAG]. The C-parameter also appears to decrease with increasing [PAG] although the error bars in Figure 5 show that the effect may be barely significant. We found that the film quantum yield increases linearly with PAG loading. This last result is not very surprising given the relationship between acid formation and [PAG] shown in eqn 1.

$$\text{Number of acids generated in film} = [\text{PAG}](1 - e^{-CE})(6.02 \times 10^{23}) \quad (1)$$

Where, C = C-parameter, and E = dose.

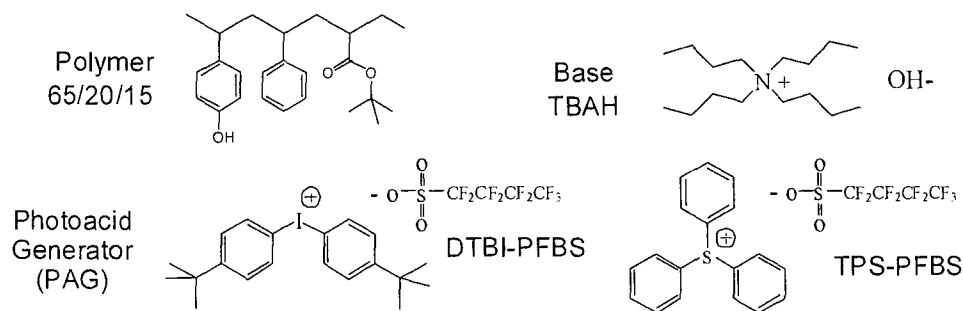


Figure 4. ESCAP resist components described previously as LUVR-99204 or LUVR-99258.¹⁵⁻¹⁸

Base %	PAG %		
	5	7.5	10
0	0.5	0.4	0.35
0.17	1.4	1.2	0.95
0.34	3.4	2.4	1.9
0.5	4.6	3.7	2.9

Table 4. Clearing doses of Platform 4 resists as a function of PAG and base loading.

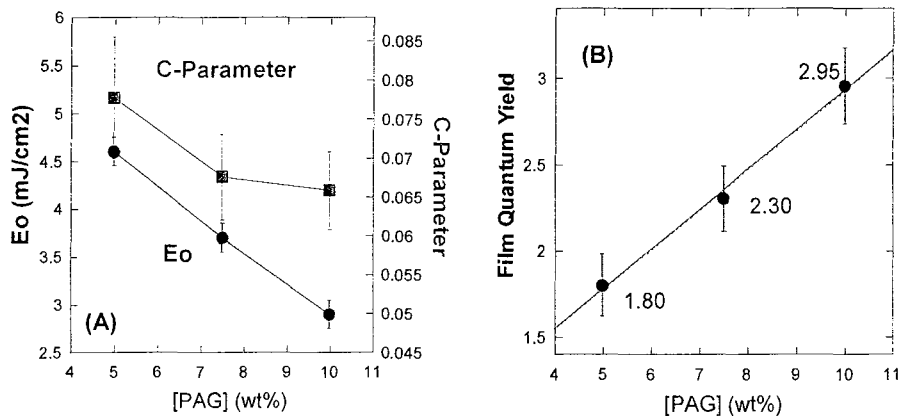


Figure 5. Relationship between C-parameters, film quantum yield as a function of the PAG concentration.

2.3 Ultrahigh PAG Resists

2.3.1 Hypothesis: PAG Titration to determine number of photoelectrons. One area of interest for our group is the determination of the number of photoelectrons generated during the exposure of chemically amplified resists to EUV radiation. Since the result shown in Figure 5 shows that a doubling of [PAG] nearly doubles the FQY, we concluded that the PAG is the limiting reagent in the reaction between photoelectrons and PAGs (eqn 2). Therefore, we asked two hypothetical questions: (1) Would it be possible to increase the loading of PAG to the point where photoelectrons become the limiting reagent; and if so, (2) Could we then use the resulting film quantum yield vs. [PAG] as a way to determine the number of photoelectrons generated (Figure 6)?



We prepared several resists using the iodonium and sulfonium PAGs (Figure 4) with loadings from 5 to 70%, then tested their coating quality, outgassing, and unexposed film thickness loss (UFTL, Table 5). All ESCAP with TPS-PFBS exhibited good coatings, even with as much as 70% PAG loading, while those with TBPI-PFBS exhibited good coatings up to 40% PAG. Resists prepared with 50% PAG gave poor coatings.

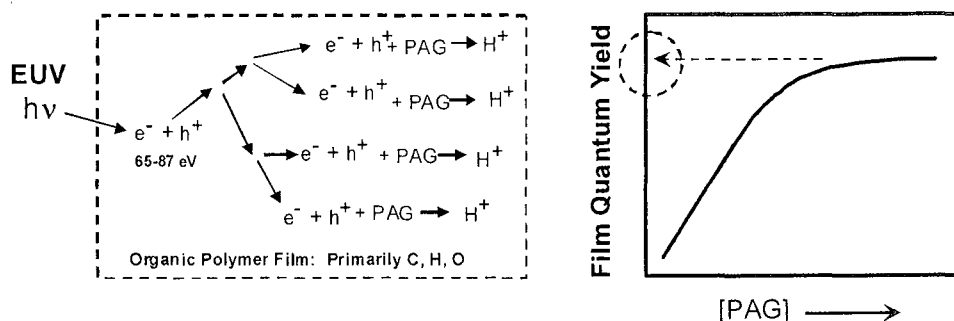


Figure 6. (A) Photoelectron cascade mechanism for EUV exposure. (B) Hypothesis prompting the investigation into effect of ultrahigh levels of PAG on Film Quantum Yield as a way to determine the number of photoelectrons generated during EUV exposure.

2.3.2 Unexposed Film Thickness Loss (UFTL). Before performing imaging experiments, we evaluated the ultrahigh PAG formulations for UFTL or dark-loss performance. Resist films prepared with 15-50% iodonium PAG (TBPI-PFBS) and 15-70% sulfonium (TPS-PFBS) PAGs were coated and baked using PAB and PEB conditions (130 °C/60s followed by 130 °C/90s) and film thickness was measured before and after 45 s development in either 0.26 or 0.13 N tetramethylammonium hydroxide (TMAH). UFTL results are shown in Table 5 and Figure 7. All of the iodonium resists showed acceptable UFTLs of 6-17 Å. The resist films prepared with the sulfonium PAG tend to have much greater UFTL values. Only the diluted 0.13 N developer gave acceptable UFTLs and only when the level of sulfonium PAG was less than 50%. During imaging experiments, all resists prepared with sulfonium PAGs were developed using 0.13 N TMAH.

% PAG	Iodonium PAG, TBPI-PFBS				Sulfonium PAG, TPS-PFBS			
	Name	Coat. Qual.	UFTL, Å 0.26 N	UFTL, Å 0.13 N	Name	Coat. Qual.	UFTL, Å 0.26 N	UFTL, Å 0.13 N
5	OS2	Good				Good		
7.5	OS1	Good			OS-S1	Good		
10	OS3	Good				Good		
15	OS4	Good	17.39	6.17	OS-S2	Good	314.97	11.14
20	OS5	Good	13.76	6.3		Good	318.21	13.1
25	OS6	Good	13.52	5.97	OS-S3	Good	376.64	17
30	OS7	Good	12.42	7.18	OS-S4	Good	500.87	21.19
40	OS8	Good		8.71	OS-S5	Good	960.9	82.78
50	OS9	Poor	10.65	7.91	OS-S6	Good	1247.7	216.58
60	OS10	Poor			OS-S7	Good	1247.9	547.17
70	OS11	Poor			OS-S8	Good	1246.4	730.82

Table 5. Coating and Unexposed Film Thickness Loss (UFTL) observed for Ultrahigh PAG resists.

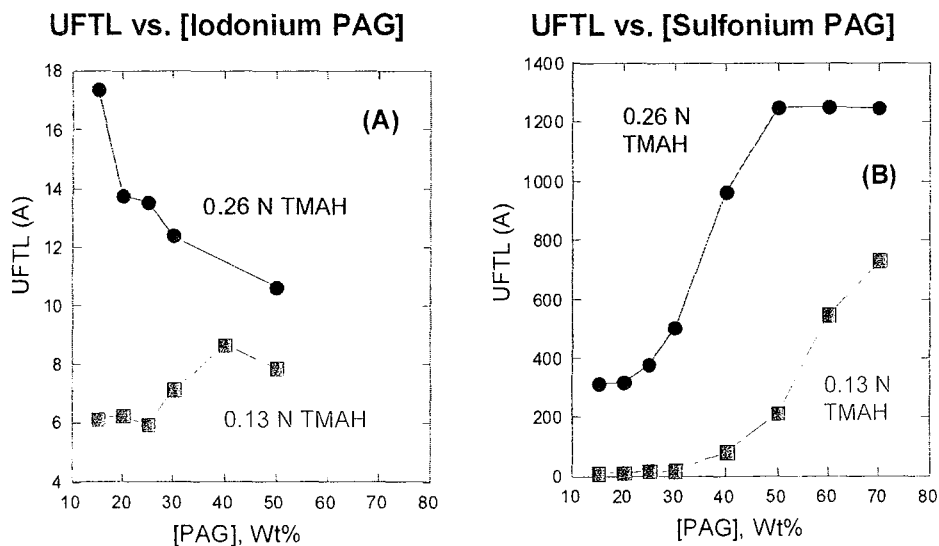


Figure 7. Plot of the ratio of unexposed film thickness loss vs. PAG concentrations. (A) UFTL as a function of iodonium PAG (TBPI-PFBS) (B) UFTL as a function of sulfonium PAG (TPS-PFBS).

2.3.3 Outgassing Tests. Outgassing measurements for ultrahigh iodonium and sulphonium PAG resists (7.5, 25 & 40 wt%) were carried out using the EUV ROX tool at CNSE (Table 6). The typical procedure is to expose resist films to 2.5x the clearing dose (E_0). Surprisingly, all resists passed the SEMATECH limit of 6.5×10^{14} molecules/cm², even in when the resists were dosed with 7x E_0 . Based on these results, we were able to perform exposure experiments on the AMET and BMET.

PAG	PAG (wt %)	2.5 x E_0	3 x E_0	7 x E_0
Iodonium TBPI-PFBS	25	2×10^{14}	2×10^{14}	4×10^{14}
	40	3×10^{14}	NA	NA
Sulfonium TPS-PFBS	25	2×10^{14}	3×10^{14}	5×10^{14}
	40	4×10^{14}	NA	NA

Table 6. Outgassing Results from resists prepared with ESCAP Terpolymer (Figure 4) and either Iodonium TBPI-PFBS or Sulfonium TPS-PFBS PAGs. Outgassing values are reported in molecules/cm² for atomic mass units of 35-200, but without 44 AMU.

2.3.4 Eos, C-Parameters and Film Quantum Yields. Based on coating quality, outgassing and UFTL performance, we selected seven resists using the iodonium PAG and three resists using the sulfonium PAG (Table 7). We plotted the clearing doses for all resists prepared with a constant amount of base (0.5% TBAH) in Figure 8A. Clearing doses determined on the Berkeley MET were reduced by a factor of 1.9 according to recent calibration results.²¹ AMET clearing doses are reported as received. All clearing doses decrease with increasing [PAG], as expected. Exposures conducted with the iodonium PAGs were conducted using both the AMET and the BMET and are in good agreement. Resists prepared with sulfonium PAGs are slightly slower than those prepared with iodonium PAGs.

Figure 8B shows the C-parameter for the resists prepared with iodonium and sulfonium PAGs as a function of PAG loading. The C-parameters for resists prepared with iodonium PAGs decrease with increasing PAG up to about 0.35 \underline{M} PAG, thereafter, the C-parameters increase. The C-parameters for resists prepared with sulfonium PAGs show a significant decrease with increasing PAG concentration.

Figure 9 shows the film quantum yield as a function of PAG concentration. The resists prepared with sulfonium PAGs reach a maximum FQY of 4.3 acids/photon absorbed, and exhibit the curvature predicted in our original hypothesis, shown in Figure 6. Since there are only three points in this curve, however, we will hold off on drawing conclusions about the implications regarding the number of photoelectrons until more detailed experiments can be conducted.

Resists prepared with iodonium PAGs do not appear to reach a limiting value as predicted (Figure 6) and as shown with sulfonium PAGs. Instead, the film quantum yields accelerate above concentrations of 0.35 \underline{M} . The resists prepared with sulfonium PAGs and with relatively low levels of iodonium PAGs (< 0.35 \underline{M}) appear to behave similarly—the C-parameters decrease with increasing [PAG] and the film quantum yields increase monotonically up to PAG concentrations of ~0.35 \underline{M} . However, at concentrations above 0.35 \underline{M} , the behaviors of the two types of PAG

diverge. The FQY of the sulfonium PAGs level off, whereas the resists prepared from iodonium PAGs accelerate reaching the highest know film quantum yields of 8-13 acids/photos absorbed. The range in these values of FQY arises due to the differences between the AMET and BMET exposure tools. Despite the differences in results between the two microexposure tools, one conclusion is clear—the iodonium PAGs appear to generate acid by a mechanism that differs from that of the sulfonium PAG when the concentration of the PAG is very high ($> 0.35 \text{ M}$).

Experiment	Resist	PAG wt%	[PAG], M	Eo 0.5% Base	Density (g/cm ³)	ABS (1-T)	Corr C	Film Quantum Yield	QY Error
OLD AMET	OS2	5	0.083	4.6	1.15	0.40	0.078	1.80	0.19
	OS1	7.5	0.123	3.7	1.13	0.40	0.068	2.31	0.20
	OS3	10	0.166	2.9	1.15	0.41	0.066	2.99	0.25
NEW AMET	OS4	15	0.247	2.4	1.14	0.42	0.054	3.53	0.15
	OS5	20	0.330	2.3	1.14	0.43	0.039	3.29	0.29
	OS7	30	0.532	1.7	1.23	0.51	0.043	4.96	0.18
	OS8	40	0.697	1.4	1.21	0.50	0.056	8.71	0.62
BMET I+	OS1	7.5	0.124	3.2	1.15	0.40	0.084	2.87	0.15
	OS4	15	0.247	2.4	1.14	0.42	0.055	3.59	0.17
	OS5	20	0.330	1.9	1.14	0.43	0.045	3.82	0.23
	OS7	30	0.532	1.7	1.23	0.51	0.052	6.08	0.33
	OS8	40	0.697	1.7	1.21	0.50	0.081	12.50	2.11
BMET S+	OS-S1	7.5	0.153	3.9	1.15	0.40	0.054	2.32	0.19
	OS-S2	15	0.307	2.8	1.15	0.41	0.043	3.55	0.35
	OS-S4	30	0.614	2.1	1.15	0.44	0.027	4.27	0.24

Table 7. Imaging and film quantum yields of Ultrahigh PAG Photoresists.

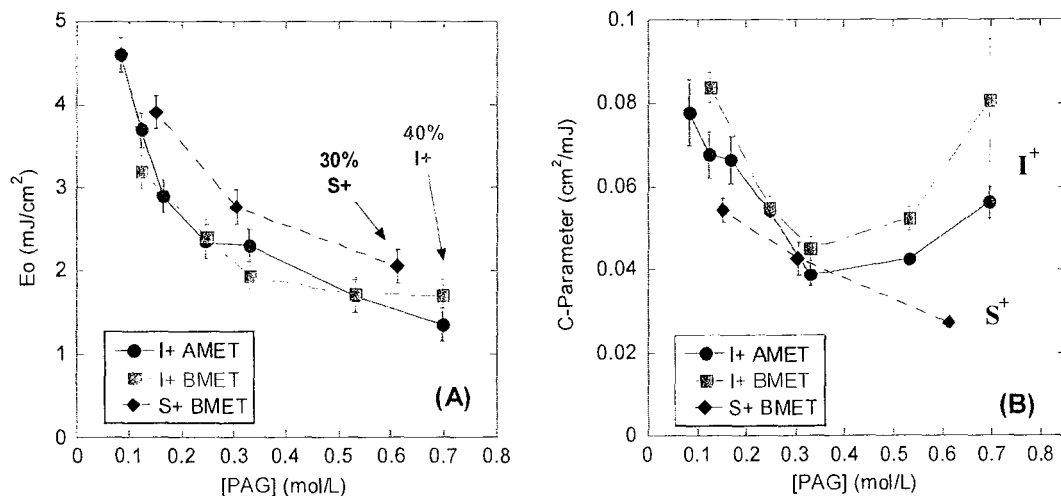


Figure 8. (A) Clearing doses vs. PAG concentration at constant base (0.5% TBAH). (B) C-Parameters vs. PAG concentration.

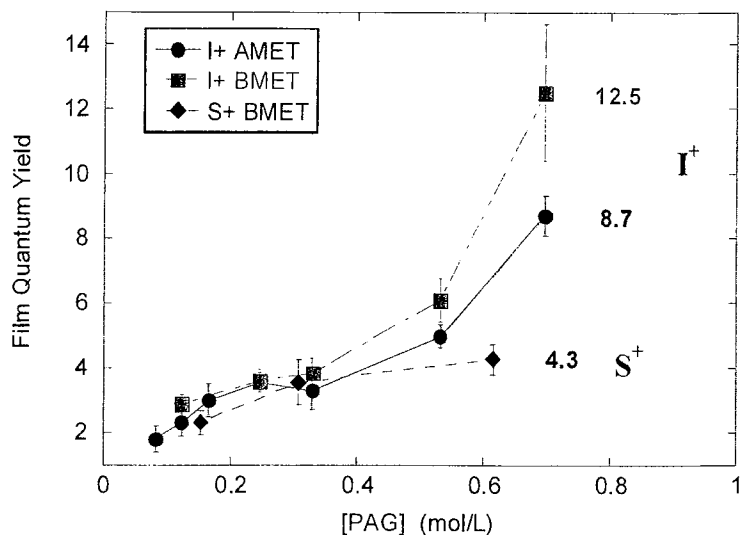


Figure 9. Film Quantum Yield vs. PAG concentration.

3. CONCLUSIONS

We used base titration methods to determine C-parameters and film quantum yield (FQY) for three industrial EUV photoresist platforms (EUV-2D, MET-2D, XP5496) and twenty academic EUV photoresist platforms. X-ray reflectometry was used to measure the film density leading to the determination of absorbance. EUV exposures at Albany and Berkeley were used to determine C-parameters leading to FQYs. Our work with four resist platforms was in support of Gallatin's RLS modeling work. We formulated photoresists with ultrahigh concentrations of iodonium sulfonium PAGs to determine the potential of these new resists to beat the RLS trade-off and to gain further insight into the EUV exposure mechanism.

We found that it is possible to reach a film quantum yield as high as 4.3 acid/absorbed photon for resists prepared with 30% sulfonium PAG, but that the FQY appears to level-off at concentrations of $\sim 0.35 \text{ M}$ sulfonium PAG. The C-parameter of resists prepared with ultrahigh concentrations of iodonium PAGs first decreases with [PAG], but then increases dramatically above $\sim 0.35 \text{ M}$ concentrations of PAG. The FQY reaches a maximum of 8-13 acids generated / photons absorbed when the concentration of PAG is 40 wt%. This is the highest quantum yield yet described for an EUV photoresist. We think that EUV resists prepared with ultrahigh levels of PAG show great potential as a pathway to improve resolution, LER and sensitivity simultaneously, and we will continue our work with these interesting materials.

4. EXPERIMENTAL

4.1 Materials. Resists for platforms 1-3 were received from Rohm and Haas Microelectronics and were based on EUV-2D (XP5435D), MET-2D (XP5271D) and XP5496F formulations, respectively. The published resists (OS resist), chemically amplified resist (CA), were composed of ESCAP terpolymers with either Di(4-*tert*-butylphenyl)iodonium perfluoro-1-butanefulfonate (DTBI-PFBS) or Triphenylsulfonium perfluoro-1-butanefulfonate (TPS-PFBS) as a PAG, tetrabutylammonium hydroxide base (TBAH), and 50/50 mixture solvent of ethyl lactate (EL) and propylene glycol methyl ether acetate (PGMEA). The ESCAP terpolymers were received from duPont Electronic Materials and were composed of 4-hydroxystyrene/styrene/*t*-butyl acrylate with 65/15/20 molar ratio, respectively. DTBI-PFBS and TPS-PFBS used in this study were purchased from Toyo Gosei. Initially, we formulated OS resists at different PAG levels based on solid from low (5, 7.5, and 10%) to high (15, 20, 25, 30, 40, 50, 60, and 70% of resist solid), all at 0.5% TBAH loading. After we optimized the resist formulations based on the coating quality, outgassing testing, and dark film loss studies, we selected DTBI-PFBS loadings at 5, 7.5, 10, 15, 20, 30, 40% and TPS-PFBS at 7.5, 15, and 30%. For each of this PAG concentration we prepared a series of OS resists containing different base TBAH loadings. In all cases, the molar concentration of the base was kept to less than 15% of that of the PAG.

4.2 Cleanroom Processing. Unless otherwise noted, photoresist samples were spin-coated on initially primed eight-inch silicon wafers and subjected to post apply bake (PAB) to yield the film thickness of interest. The resist-coated wafer then exposed, subjected to a post-exposure bake (PEB) and finally developed utilizing single puddle of standard MF26A™ for 45 seconds. For TPS-PFBS OS-Type resists we used 50/50 diluted MF26A™. Processing conditions for each platform are as follows. For XP5496 series: PAB: 110 °C/60 s yielding film thickness (FT): 80 nm, PEB: 110 °C/90 s. For MET-2D PAB: 120 °C/60 s at FT: 80nm, PEB: 130 °C/90 s. Both EUV-2D and OS; PAB: 130 °C/60 s FT: 125 nm, PEB: 130 °C/90 s.

Exposures were performed at two different Sematech facilities: Albany EUV microexposure tool (AMET) and Berkeley EUV microexposure tool (BMET). The dose-to-clear for each resist and contrast curves (CCs) were evaluated initially at AMET utilizing 10X10 experimentally array for this experiment. AMET tool was operated at open field condition only (no mask). The later CCs for OS resists were determined at BMET tool. OS resists at 5, 7.5, 10% DTBI-PFBS loadings were also imaged using dense line patterns at EUV BMET targeting possible process windows for both resolution and LER. BMET tool with numerical aperture (NA) of 0.25 was operated at annular conditions for these resists. Finally, we did outgassing testing for some OS resists having low and ultrahigh DTBI-PFBS or TPS-PFBS concentrations using ROX EUV at CNSE, Albany.

4.3 X-ray Reflectivity Film Density Measurements. Film densities were determined using specular X-ray reflectometry analyses performed using a Bruker D8 Discover high resolution diffractometer operated in a θ - θ geometry. X-rays from the line focus of a sealed copper tube were conditioned by a graded parabolic X-ray multilayer mirror before being diffracted by a two-reflection V-groove beam compressor. The beam conditioner produced a monochromatic Cu $K\alpha_1$ incident X-ray beam with approximate dimensions of 10 mm by 220 μ m. The specularly reflected incident beam was conditioned in angle by a 0.2 mm slit before being detected by a scintillation counter. Absorbers in the incident beam were used to automatically maintain the reflected intensity within the linear regime of the detector at all times. A knife-edge was positioned normal to the sample surface to intercept approximately 50% of the X-ray beam propagating parallel to the surface at $2\theta = 0$; this permitted the reliable observation of the specular reflection profile below the critical angle for total external reflection from the photoresist layer. Specular XRR intensities were recorded using a step size of 0.005° out to 8° 2θ , where all intensity oscillations arising from the photoresist film thickness were damped out by the effects of interfacial roughness. Following data collection, the specular XRR data were analyzed using the Bruker LEPTOS software package.

4.4 C-Parameters and Film Quantum Yield. EUV film quantum yields were determined by systematic measurements for each resist platform. A series of 4-5 resist samples that are identical except with different base loadings were exposed to EUV radiation in order to establish the clearing doses, E_0 's. The [base]/[PAG] ratio spanned over 0.0-0.25. The data was analyzed using the C-parameter (C) method developed by Szmanda et. al.¹⁴ and the quantum yield method developed by us.⁵ In this study, the C-parameter was determined by plotting of [base]/[PAG] ratio vs. EUV E_0 resulting in linear response. To determine C, initial slope of the obtained line from this plot was corrected for the EUV attenuation utilizing the film absorbance (a) in base units:

$$C = slope \cdot \frac{a}{(1 - e^{-a})}$$

Using the measured C, the number of acid generated after EUV exposures was calculated from Equation 1. To compute the resist absorbance at EUV we used CXRO Website that based on atomic absorbance parameters.²² The empirical formulas for each parent resist were used in combination with film density determined by small angle X-ray reflectometry. Combined with optical density information, we were able to calculate the number of Photons Absorbed and determine film quantum yield (Figure 2).

5. ACKNOWLEDGEMENTS

We thank Sematech for financial support and duPont Electronic Materials for supplying the polymer shown in Figure 4. This work was supported by the Director, Office of Science, of the U.S. Department of Energy under Contract No. DE-AC02-05CH11231.

Disclaimer:

Advanced Materials Research Center, AMRC, International SEMATECH Manufacturing Initiative, and ISMI are servicemarks of SEMATECH, Inc. SEMATECH, and SEMATECH logos are registered servicemarks of SEMATECH, Inc. All other servicemarks and trademarks are the property of their respective owners.

6. NOTES and REFERENCES

- [1] Resist performance has been named one of the three most critical barriers to successful implementation of EUV lithography during the last four annual EUV Lithography Symposiums.
- [2] Gallatin, G. M., Proc. SPIE, 5753, 38-52 (2005).
- [3] Gallatin, G. M., Naulleau, P., Brainard, R., "Fundamental limits to EUV photoresist," Proc. SPIE, 6519, 651911/1-651911/10. (2007).
- [4] Gallatin, G. M., Naulleau, P., Brainard, R., Niakoula, D. and Dean, K., "Resolution, LER and Sensitivity Limitations of Photoresists," EUV Symposium, Sapporo, Jpn (2007).
- [5] Brainard, R., Trefonas, P., Lammers, J., Cutler, C., Mackevich, J., Trefonas, A. and Robertson, S., Proc. SPIE, 5374, 74-85 (2004).
- [6] Brainard, R. L., Henderson, C., Cobb, J., Rao, V., Mackevich, J. F., Okoroanyanwu, U., Gunn, S., Chambers, J. and Connolly, S., "Comparison of the lithographic properties of positive resists upon exposure to deep- and extreme-ultraviolet radiation," Journal of Vacuum Science & Technology, B: Microelectronics and Nanometer Structures, 17(6), 3384-3389 (1999).
- [7] Brainard, R. L., Barclay, G. G., Anderson, E. H., Ocola, L. E., "Resists for next generation lithography," Microelectronic Engineering, 61-62, 707-715 (2002).
- [8] Kozawa, T., Tagawa, S., "Basic aspects of acid generation processes in chemically amplified resists for electron beam lithography," Proc. SPIE 5753(Pt. 1, Advances in Resist Technology and Processing XXII), 361-367 (2005). Kozawa, T., Tagawa, S., "Basic aspects of acid generation processes in chemically amplified electron beam resist," Journal of Photopolymer Science and Technology, 18(4), 471-474 (2005).
- [9] Tagawa, S., Nagahara, S., Iwamoto, T., Wakita, M., Kozawa, T., Yamamoto, Y., Werst, D. and Trifunac, A. D., "Radiation and photochemistry of onium salt acid generators in chemically amplified resists," Proc. of SPIE-The International Society for Optical Engineering, 3999(Pt. 1, Advances in Resist Technology and Processing XVII), 204-213 (2000).

- [10] Nakano, A., Okamoto, K., Yamamoto, Y., Kozawa, T., Tagawa, S., Kai, T., Nemoto, H., Shimokawa, T., "Deprotonation mechanism of poly(4-hydroxystyrene) and its derivative," Proc. of SPIE-The International Society for Optical Engineering, 5753(Pt. 2, Advances in Resist Technology and Processing XXII), 1034-1039 (2005).
- [11] Kozawa, T., Saeki, A., Tagawa, S., "Modeling and simulation of chemically amplified electron beam, x-ray, and EUV resist processes." Journal of Vacuum Science & Technology, B: Microelectronics and Nanometer Structures--Processing, Measurement, and Phenomena, 22(6), 3489-3492 (2004).
- [12] Yamamoto, H., Kozawa, T., Nakano, A., Okamoto, K., Tagawa, S., Ando, T., Sato, M., Komano, H., "Dependence of acid generation efficiency on the protection ratio of hydroxyl groups in chemically amplified electron beam, x-ray and EUV resists," Journal of Vacuum Science & Technology, B: Microelectronics and Nanometer Structures--Processing, Measurement, and Phenomena, 22(6), 3522-3524 (2004).
- [13] Kozawa, T., Saeki, A., Nakano, A., Yoshida, Y., Tagawa, S., "Relation between spatial resolution and reaction mechanism of chemically amplified resists for electron beam lithography," Journal of Vacuum Science & Technology, B: Microelectronics and Nanometer Structures--Processing, Measurement, and Phenomena, 21(6), 3149-3152 (2003).
- [14] Szmanda, C. R., Brainard, R. L., Mackevich, J. F., Awaji, A., Tanaka, T., Yamada, Y., Bohland, J., Tedesco, S., Dal'Zotto, B., Bruenger, W., Torkler, M., Fallmann, W., Loeschner, H., Kaesmaier, R., Nealey, P. M., Pawloski, A. R., "Measuring acid generation efficiency in chemically amplified resists with all three beams," Journal of Vacuum Science & Technology, B: Microelectronics and Nanometer Structures, 17(6), 3356-3361 (1999).
- [15] Roberts, J. M., Meagley, R., Fedynyshyn, T. H., Sinta, R. F., Astolfi, D. K., Goodman, R. B., Cabral, A., "Contributions to innate material roughness in resist," Proc. of SPIE, 6153, 61533U/1-61533U/11 (2006).
- [16] Fedynyshyn, T.H., Astolfi, D. K., Cabral, A. and Roberts, J., "PAG segregation during exposure affecting innate material roughness," Proc. SPIE, 6519, 65190X (2007).
- [17] Woodward, J. T., Fedynyshyn, T. H., Astolfi, D. K., Cann, S., Roberts, J. M., Leeson, M. J., "Component segregation in model chemically amplified resists," Proc. of SPIE, 6519, 651915/1-651915/8 (2007).
- [18] Fedynyshyn, T. H., Pottebaum, I., Cabral, A., Roberts, J., "Changes in resist glass transition temperatures due to exposure," Proc. of SPIE, 6519, 651917/1-651917/12 (2007).
- [19] Patrick Naulleau, personal communication.
- [20] Chandhok, M., Cao, H., Wang, Y., Gullikson, E. M., Brainard, R. L., Robertson, S. A., "Techniques for directly measuring the absorbance of photoresists at EUV wavelengths," Proc. of SPIE, 5374(Pt. 2, Emerging Lithographic Technologies VIII), 861-868 (2004).
- [21] Contrast curve experiments were conducted during January 2008. Patrick Naulleau announced during the EUVI Resist workshop, SPIE 2/28, to bring exposures in line with recent calibration experiments, doses determined prior to 2/28 should be divided by 1.9.
- [22] CXRO website: http://henke.lbl.gov/optical_constants. Also see: Henke, B. L., Gullikson, E. M. and Davis, J. C., "X-ray interactions: photoabsorption, scattering, transmission, and reflection at E=50-30000 eV, Z=1-92," Atomic Data and Nuclear Data Tables Vol. 54 (no.2), 181-342 (July 1993).